AIMS Mathematics, 10(9): 22622–22649.
DOI: 10.3934/math.20251007
Received: 21 July 2025
Revised: 07 September 2025
Accepted: 22 September 2025
Published: 29 September 2025

https://www.aimspress.com/journal/Math

Research article

On the pricing of double barrier options under stochastic volatility models: A probabilistic approach

Jerome Detemple[1], **Yerkin Kitapbayev**[2,*] **and Danila Shabalin**[3,4]

[1] Questrom School of Business, Boston University, Boston, MA 02215, USA
[2] Mathematics Department, Khalifa University of Science and Technology, P.O. Box 127788, Abu Dhabi, United Arab Emirates
[3] Faculty of Mechanics and Mathematics, Lomonosov Moscow State University, Moscow, Russia
[4] Vega Institute Foundation, Moscow 119234, Russia

* **Correspondence:** Email: yerkin.kitapbayev@ku.ac.ae.

Abstract: We study the pricing of double barrier knock-out options under stochastic volatility using a conditional Monte Carlo method based on the local time-space formula of Peskir. A valuation formula including an early knock-out discount is provided, where the discount depends on the local time of the underlying stochastic processes and the deltas of the option at the barriers. The latter solve a system of coupled Volterra integral equations of the first kind. This characterization leads to an efficient numerical method for general volatility diffusion models. An algorithm for numerical implementation, based on a conditional quasi-Monte Carlo simulation method, is presented and shown to converge numerically to the true value of the claim. A numerical study is performed to illustrate properties of double barrier knock-out calls in the Heston stochastic volatility model. In our calibration, we find that short-dated (long-dated) at-the-money (ATM) knock-out call prices increase (decrease) when the speed of mean reversion increases, long run mean volatility increases, and vol-of-vol decreases. We also find that the deltas and vegas of short-dated ATM double barrier calls can be very sensitive to volatility in contrast to long-dated ones.

Keywords: barrier option; Volterra integral equation; local time; stochastic volatility model; Monte-Carlo method
Mathematics Subject Classification: 60H30, 60J55, 91G20, 91G60

1. Introduction

A barrier option is a path-dependent derivative whose payoff depends on the crossing of a barrier. A knock-out barrier option is a contract that expires at the first time a pre-specified barrier is breached.

A double barrier knock-out option expires at the crossing of either of two pre-specified barriers. The barriers can be constants or functions of time. Expiration can entail the payment of a rebate, i.e., a terminal cash payment. Barrier options are traded in the over-the-counter (OTC) market. They are especially common in foreign exchange (FX) markets where they are used to manage currency risks; see [45]. In this paper, we study the valuation of single and double barrier options when the underlying asset price has a stochastic volatility coefficient which follows a diffusion process.

Our contribution is threefold. First, we derive a new valuation formula for the price of a double barrier knock-out option, when the underlying asset price has a stochastic volatility modeled as a diffusion process and the interest rate and dividend yield are time-dependent functions. We show that the double barrier option price is the value of a European double barrier option reduced by a discount for early knockout (EKD), i.e., for breach of the barrier prior to the maturity date. In this two-state-variables setting, both the European component and the EKD depend on the underlying price and the volatility. The EKD is parameterized by the two deltas of the contract at the knock-out barriers. The latter, which depend on volatility, satisfy a system of coupled Volterra integral equations (VIEs) of the first kind.

Second, we present an algorithm for numerical computation. To implement the pricing formula, we first need to solve the system of VIEs for the deltas at the barriers. The algorithm proceeds recursively. At each step of the discretized time interval, and at each point of a volatility grid, it numerically computes the deltas, based on already-known future deltas. For computation of the expectation of the recursive component of the VIEs, we use a conditional quasi-Monte Carlo simulation method implemented via low discrepancy sequences (Sobol or Halton) and a Brownian bridge construction with midpoint refinement ([6]). For future values of deltas, we interpolate over the future values at the grid points. Numerical experiments illustrate the convergence of the algorithm to the true values of the claims considered when the underlying price follows a geometric Brownian motion (GBM) or a conditional GBM with mean-reverting square root volatility (CGBM-MRSRV). They also illustrate the improved convergence rate relative to a plain Monte Carlo approach.

The last contribution is on the economic front. We conduct a numerical study to provide new insights about the value of a double barrier knock-out call option with null rebate. Assuming volatility follows a mean-reverting square root process, as in [19], we document the behavior over time of the delta hedges at the barriers. We also examine the impact on the price of the speed of mean reversion, the long run mean volatility, and the volatility of volatility (vol-of-vol) parameter. Long- and short-dated at-the-money (ATM) knock-out call prices are found to respond in opposite directions, reflecting conflicting effects on the likelihood of early knock-out and on the risk incentives associated with the convexity/concavity of conditional call prices with respect to price and volatility. The responses of ATM double barrier knock-out call prices are distinct from the responses of ATM single barrier knock-out call prices which display uniform variations independent of time-to-maturity in our calibration. Finally, deltas and vegas of short-dated ATM double barrier calls tend to exhibit stronger responses to volatility changes in comparison to ATM single barrier and long-dated ATM double barrier deltas and vegas.

The paper relates to several branches of the derivatives' literature. First, it connects directly with recent contributions on the valuation and hedging of double barrier options under one-dimensional diffusion models, notably [16, 22, 35]. All of these references derive VIEs for the deltas of double barrier options. The first one studies the valuation of time-dependent double barrier derivatives when

the underlying price follows a diffusion process with linear drift. It derives a system of VIEs for the deltas of the contract at the barriers. The second one provides integral representations for barrier options using the Mellin transforms of auxiliary functions, assuming the underlying price follows a linear diffusion with time-dependent coefficients. It shows the auxiliary functions satisfy Volterra equations of the first kind. The last one proves VIEs for the deltas of a double barrier option with time-dependent barriers when the underlying follows a general diffusion with time-dependent coefficients. Derivations rely on the general integral transform method and the heat potential method. We contribute to this literature by extending the analysis to stochastic volatility models where volatility follows a diffusion process. We derive valuation formulas as well as VIEs for the deltas at the barriers in this context and provide a numerical method based on a conditional quasi-Monte Carlo simulation approach for implementation. We provide theoretical results on the existence and uniqueness of the solutions to the VIEs, and on the convergence of the scheme.

Second, it relates to a broad literature on the valuation of barrier options, a topic of long-standing interest in finance. Valuation formulas for single barrier options already appear in [34]. [27] establishes a pricing formula for a double barrier knock-out option with curved barriers taking the form of a sum of an infinite series of weighted normal distributions. [14] develops pricing and hedging formulas for double barrier options based on the inversion of the Laplace transform of the price with respect to the maturity date. [37] prices double barrier options using the inverse of the Laplace transform of the probability density function. [32] uses a Fourier series expansion. [4] develops a numerical algorithm based on Carr's randomization method. [36] presents an algorithm based on a continuous time Markov chain approximation, when the underlying price follows a Markov process. [7] prices single barrier options when the underlying follows a time-dependent Ornstein-Uhlenbeck process. The authors obtain valuation formulas by applying the general integral transform and the heat potential method. The latter method goes back to [30]; see also the generalization to the Bessel equation in [8]. The former is used in [9, 21]. A heat potential method combined with Monte Carlo simulation is also used by [31] to price single barrier options in the Heston model. The core of this approach appears in [33] which uses a finite difference method to price the option given a trajectory of volatility.

Third, it also connects to the literature on the valuation of claims under stochastic volatility. Fundamental contributions by [20] and [19] establish valuation formulas for GBM and MRSR volatility processes, respectively. [3] extends the Heston model to allow for jumps. Applications to barrier options include [11] which uses a method of lines, [15] which proposes a semi-analytic pricing approach based on the boundary element method, [23] which uses asymptotic expansion and Mellin transform methods, [46] which develops an efficient Monte Carlo scheme, [13] which employs a second-order truncation of the infinite Wiener–Itô chaos series expansion of the underlying price, and [24] which combines a singular perturbation method with a double Mellin transform and the method of images to obtain a price approximation. Our contribution to this literature is to derive novel representation formulas for single and double barrier options when volatility follows an arbitrary diffusion process and to propose an associated computational method.

Fourth, it relates to recent developments in the area dealing with alternative specifications for underlying processes or more complex types of barrier contracts. [47] prices barrier options in regime switching models using matrix Wiener-Hopf factorizations and Fourier transforms to obtain integral representations—enhancing both accuracy and computational tractability, [28] assumes a two-scale stochastic volatility process driven by a pair of approximate fractional Brownian motions and uses

Mellin transforms to derive approximate closed-form expressions for barrier option prices—facilitating faster approximation and insights into volatility scaling, and [18] prices timer barrier options in Heston's model providing analytical formulas via the method of images—a powerful technique to simplify barrier problems into more tractable forms. [17] derives exact valuation formulas for single barrier options with stochastic outside and window barriers, incorporating stochastic interest rates and jumps in the underlying process—providing analytical expressions that are both tractable and directly implementable. A critical ingredient in this derivation is the independence of the knockout time from the interest rate. [25] prices return barrier options and examines their properties in five FX model families, namely Levy, jump-diffusions, stochastic volatility, stochastic volatility with jumps, and stochastic local volatility models. For computation and calibration the authors use Fourier transforms, Monte Carlo simulation, or asymptotic expansion methods. Pricing and calibration are also carried out in [1] focusing on a Heston-Kou model with MRSR volatility and double exponential jumps. The authors demonstrate the model's superior calibration and pricing performance across a range of exotics, including barrier options, employing Fourier techniques (PROJ method) and provide a publicly available code.

Lastly, the analysis relies on the local time-space calculus, developed by [38], for continuous piecewise smooth functions of a semi-martingale. An application of this calculus to the valuation of plain vanilla American options appears in [39] and to the valuation of corporate debt in [12]. Here, we use the method to derive a valuation formula for a double barrier call option with null rebate, which has a discontinuous terminal payoff at the upper barrier. We then employ that formula to deduce a system of coupled VIEs of the first kind for the deltas of the contract at the barriers. The interest of this approach is that VIEs naturally capture the boundary behavior of the option price in a diffusion setting with two state variables, here the underlying stock price and its volatility. The downside of PDEs, in comparison, is that adapting PDE solvers to stochastic volatility leads to high-dimensional systems. While Mellin and Fourier transform methods are efficient, they are less adaptable beyond affine volatility models.

Sections 2 and 3 review the valuation of single barrier options when the underlying asset return has constant and time-dependent parameters, respectively. Section 4 describes the approach for stochastic volatility. The valuation of double barrier options is carried out in Section 5, first for the time-dependent parameter case, and then for the stochastic volatility case. Section 6 performs a numerical study to illustrate properties of double barrier options with stochastic volatility. Conclusions follow and proofs are in the Appendix.

2. Single barrier options: constant parameters

Let us assume the stock price X is modeled by a geometric Brownian motion (GBM) under the risk-neutral measure Q:

$$dX_t = (r - q)X_t dt + \sigma X_t dW_t \tag{2.1}$$

where r is the risk-free interest rate, q is the dividend yield, $\sigma > 0$ is the volatility parameter, and W is a standard Brownian motion (SBM) process under Q. We consider a down-and-out call option on X with strike K, barrier $H < X_0$, and maturity date T. We also assume that $K > H$. The price of the option $V(t, x)$ is then given by

$$V(t, x) = V_{do}(t, x) = \mathbb{E}_{t,x}\left[e^{-r(T-t)}(X_T - K)^+ I(m_T > H)|m_t > H\right] \tag{2.2}$$

for $t \in [0, T)$ and $x > H$, where the expectation is taken under Q and m_T represents the minimum of the stock price:

$$m_T = \min_{0 \le t \le T} X_t. \tag{2.3}$$

As the joint distribution of (X_T, m_T) is known in the case of constant parameters, the price $V(t, x)$ is given by

$$V(t, x) = V_e(t, x) - V_{di}(t, x) \tag{2.4}$$

for $t \in [0, T)$ and $x > H$, where V_e is the price of the standard European call option on X with the strike K and the maturity T, calculated using the Black-Scholes formula, see (2.10) below, while V_{di} is the price of a down-and-in call option:

$$V_{di}(t, x) = xe^{-q(T-t)} \left(\frac{H}{x}\right)^{2\lambda} \Phi(y) - Ke^{-r(T-t)} \left(\frac{H}{x}\right)^{2\lambda-2} \Phi\left(y - \sigma\sqrt{T-t}\right) \tag{2.5}$$

where

$$y = \frac{\log\left(\frac{H^2}{x \cdot K}\right)}{\sigma\sqrt{T-t}} + \lambda\sigma\sqrt{T-t}, \lambda = \frac{r - q + \frac{\sigma^2}{2}}{\sigma^2},$$

and $\Phi(\cdot)$ is the cumulative distribution function of the standard normal law.

Even though the explicit solution is already given above, we will now derive an alternative characterization (though it is semi-explicit) based on probabilistic arguments. Its advantage is that we can extend this method to the case of time-dependent parameters and double barrier options, unlike formula (2.4). For this, we recall that the pricing problem can be reduced to the fixed boundary PDE system

$$\frac{\partial}{\partial t} V + \mathbb{L}V = rV, \quad t \in [0, T), \quad x > H, \tag{2.6}$$

$$V(t, x) = 0, \quad t \in [0, T), \quad x \le H, \tag{2.7}$$

$$V(T, x) = (x - K)^+, \quad x > 0, \tag{2.8}$$

where $\mathbb{L}f = (r - q)xf' + \frac{1}{2}\sigma^2 x^2 f''$ is the operator of X. The following theorem provides the valuation formula for V in terms of its delta $\{V_x(t, H+), t \in [0, T)\}$ just above the barrier H. The latter is ex-ante unknown, but in the propositions below, we characterize it as the solution to a linear Volterra equation of the first kind.

Theorem 2.1. *The barrier option price can be decomposed as*

$$V(t, x) = V_e(t, x) - \frac{1}{2} \int_t^T e^{-r(u-t)} f(u) \varphi\left(d^-(x, H, u - t)\right) \frac{\sigma H}{\sqrt{u - t}} du \tag{2.9}$$

where $\varphi(x) = \frac{1}{\sqrt{2\pi}} e^{-\frac{x^2}{2}}$ is the standard normal probability density function, V_e is the price of the standard European call:

$$V_e(t, x) = xe^{-q(T-t)} \Phi\left(d^+(x, K, T - t)\right) - Ke^{-r(T-t)} \Phi\left(d^-(x, K, T - t)\right) \tag{2.10}$$

$$d^{\pm}(x, K, s) = \frac{1}{\sigma\sqrt{s}} \left(\log\frac{x}{K} + \left(r - q \pm \frac{\sigma^2}{2}\right) s\right) \tag{2.11}$$

and $f(t) := V_x(t, H+)$ is the barrier option's delta at $x = H+$ for $t \in [0, T)$.

The proof is given in the Appendix. The integral term in (2.9) corresponds to the local time term in Peskir's formula; see [38]. As mentioned above, the formula (2.9) is not self-sufficient as it contains the unknown option's delta $f(t)$. The following result characterizes $f(t)$ as the solution to a Volterra equation; the derivation can also be found in the Appendix.

Theorem 2.2. *The function $f(t)$ satisfies the linear Volterra integral equation of the first kind with weak singularity:*

$$V_e(t,H) = \int_t^T f(u)\frac{k(t,u)}{\sqrt{u-t}}du \tag{2.12}$$

for $t \in [0,T)$, where the kernel $k(t,u)$ is given by

$$k(t,u) = \frac{1}{2}e^{-r(u-t)}\varphi\left(\left(\frac{r-q}{\sigma} - \frac{\sigma}{2}\right)\sqrt{u-t}\right)\sigma H \tag{2.13}$$

for $u \geq t$. The terminal condition is $f(T-) := \lim_{t\uparrow T} f(t) = 0$.

Once the delta $f(t)$ of V at $H+$ is determined numerically, we can compute the option price using (2.9). In the following sections, we extend the methodology above to the case of time-dependent volatility and double barrier options.

Remark 2.3. *We note that, by the parity relation* (2.4) *for barrier options and Eq* (2.9)*, the price of the down-and-in call option can be written in the integral form*

$$V_{di}(t,x) = \frac{1}{2}\int_t^T e^{-r(u-t)}f(u)\varphi\left(d^-(x,H,u-t)\right)\frac{\sigma H}{\sqrt{u-t}}du \tag{2.14}$$

for $t \in [0,T)$ and $x > H$.

Now, by reversing time and applying a change of variables, we transform the Eq (2.12) into its standard forward form:

$$g(t) = \int_0^t \frac{\tilde{f}(u)\tilde{k}(t,u)}{\sqrt{t-u}}du, \quad 0 \leq t \leq T, \tag{2.15}$$

where $g(t) = V_e(T-t,H)$, $\tilde{f}(t) = f(T-t)$, $\tilde{k}(t,s) = k(T-t,T-s)$ are time-reversed functions. For equations of the form (2.15), numerous studies such as [2] have been devoted to establishing sufficient conditions for the existence and uniqueness of solutions. In our case, we shall refer to Theorem 6.1.13 stated in [5], which can be formulated as:

Theorem 2.4. *Assume that*

(a) $g(t) \in C^1([0,T])$ with $g(0) = 0$;
(b) $\tilde{k}(t,s) \in C^{1,0}([0,T]\times[0,T])$, with $|\tilde{k}(t,t)| \geq k_0 > 0$ when $t \in [0,T]$.

Then, the Volterra integral equation (2.15) *has a unique solution $\tilde{f}(t) \in C([0,T])$.*

It can be easily seen that in our case $g(t)$ and $\tilde{k}(t,s)$ are analytic functions, $g(0) = V_e(T,H) = (H-K)^+ = 0$, and

$$\tilde{k}(t,t) = \frac{\sigma H}{2\sqrt{2\pi}} > 0.$$

Solving this equation requires numerical methods. The simplest and most effective ones are those based on the product integration approach described in [29]. First, we introduce the uniform grid $\{t_i = i\Delta t,\ i = 0, 1, \ldots, m\}$ with $\Delta t = T/m$ for some m. The approximate solution for the value $\tilde{f}(t_i)$ based on this grid will be denoted by $\hat{f}_i$, $i = 0, \ldots, m$. Also assume $g_i = g(t_i)$, $\tilde{k}_{i,j} = \tilde{k}(t_i, t_j)$. Next, we approximate $\tilde{f}(u)\tilde{k}(t_i, u)$ by the piecewise linear function

$$((t_{j+1} - u)\,\tilde{k}_{i,j}\,\hat{f}_j + (u - t_j)\,\tilde{k}_{i,j+1}\,\hat{f}_{j+1})/\Delta t, \quad t_j \le u \le t_{j+1}, \quad j = 0, \ldots, i-1. \tag{2.16}$$

As a result, the integral equation (2.15) is approximated by the following lower triangular system for $\hat{f}_i$:

$$\sum_{j=1}^{i} \hat{f}_j\,\tilde{k}_{i,j}\,\omega_{i-j} = \frac{3}{4}\,g_i\,\Delta t^{-1/2}, \quad i = 1, \ldots, m, \tag{2.17}$$

where ω_{i-j} are precomputed weights: $\omega_0 = 1$ and $\omega_l = (l+1)^{3/2} - 2l^{3/2} + (l-1)^{3/2}$, $l = 1, \ldots, m-1$. According to [43], it may be shown that, under sufficient smoothness assumptions on $\tilde{f}(t)$ and the kernel $\tilde{k}(t, s)$, the convergence order of this scheme is $O(\Delta t^2)$. Since the smoothness of $\tilde{k}(t, s)$ is evident, the desired smoothness of $\tilde{f}(t)$ follows directly from Theorem 6.1.14 in [5].

Theorem 2.5. *Assume that*

(a) $g(t) \in C^{q+1}([0, T])$ *for some* $q \in \mathbb{N}$*;*
(b) $\tilde{k}(t, s) \in C^{q+1}([0, T] \times [0, T])$*, with* $|\tilde{k}(t, t)| \ge k_0 > 0$ *for all* $t \in [0, T]$*;*
(c) $g^{(r)}(0) = 0$ *for* $r = 0, 1, \ldots, p$ *where* $p < q$.

Then, the unique solution to (2.15) *belongs to the space* $C^p([0, T]) \cap C^q((0, T])$.

At this point, given the numerical solution $\hat{f}$, we can compute the price of the down-and-out call option $V(t, x)$ by performing a numerical integration in (2.9). It should be noted that there is no singularity at $u = t$ for $x > H$ as the function φ dominates the $\sqrt{u - t}$ term. Therefore, the integral can be computed using standard quadrature formulas on a grid conjugate to the discrete solution $\hat{f}_i$. In order to preserve the second-order convergence, we employ the composite trapezoidal rule. Note also that the overall algorithmic complexity to solve the VIE and compute the option price is $O(m^2)$. Table 1 illustrates the convergence of the numerical scheme for the single barrier option price as m increases, in the model with constant volatility. Figure 1 shows the behaviors of the option price and delta with respect to time.

Table 1. This table shows the convergence of the single barrier option price based on the representation (2.9) to the exact price (2.4) and (2.5) as a function of the number of time steps m in the numerical scheme. The parameters are $r = 0.05$, $\delta = 0.02$, $\sigma = 0.3$, $T = 2$, $X_0 = 100$, $K = 100$, $H = 80$.

Maturity	Exact	$m = 8$	$m = 32$	$m = 64$	$m = 128$
0.25	6.2993	6.3056	6.2999	6.2994	6.2993
0.5	8.9195	8.9446	8.9206	8.9197	8.9195
1.0	12.0871	12.0992	12.0878	12.0872	12.0871
1.5	14.0008	14.0080	14.0013	14.0008	14.0008
2.0	15.3103	15.3156	15.3107	15.3103	15.3103

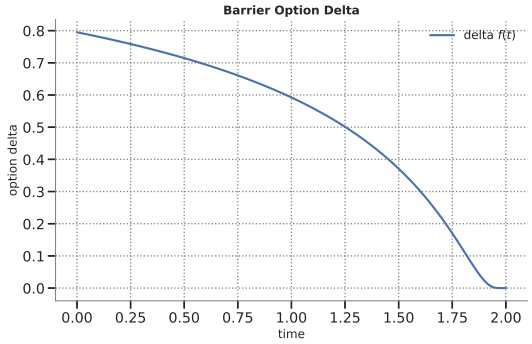

(a) single barrier option delta

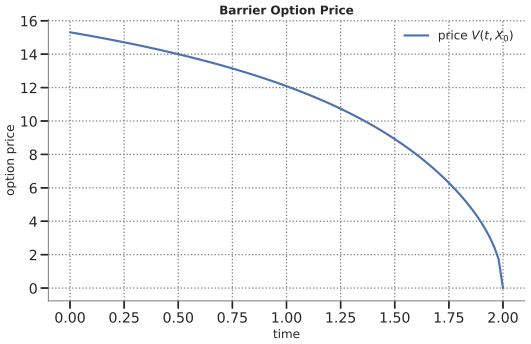

(b) single barrier option price

Figure 1. This figure displays the option's delta $f(t)$ (panel (a)) given as the solution to the equation (2.12), and the single barrier option price $V(t, X_0)$ (panel (b)) computed using (2.9), both as functions of $t \in [0, T]$. The parameters are $r = 0.05$, $\delta = 0.02$, $\sigma = 0.3$, $T = 2$, $X_0 = 100$, $K = 100$, $H = 80$.

3. Single barrier options: time-dependent parameters

In this section, the stock price X is given by a geometric Brownian motion with time-dependent parameters,* under the risk-neutral measure Q:

$$dX_t = (r(t) - q(t))X_t dt + \sigma(t)X_t dW_t \tag{3.1}$$

where $r(t)$ is the time-dependent risk-free interest rate, $q(t)$ is the time-dependent dividend yield, and $\sigma(t) > 0$ is the time-dependent volatility function. The goal again is to price a down-and-out call option on X with strike K, barrier H, and maturity date T. We note that, as we have a deterministic $\sigma(t)$, the distribution of $\log(X_t)$ is Gaussian, and hence, the results from the preceding section can be shown in almost the same fashion.

The next two theorems extend the corresponding results from the previous section. The proofs are quite similar and hence will not be repeated. To avoid additional notation, we still denote by V and V_e the prices of down-and-out and European call options, respectively, under the dynamics (3.1) of the underlying X. Also, we denote the delta of V at $x = H+$, by $f(t) := V_x(t, H+)$, $t \in [0, T)$.

Theorem 3.1. *The option price V under the dynamics* (3.1) *of X can be decomposed as*

$$V(t, x) = V_e(t, x) - \frac{1}{2}\int_t^T e^{-\int_t^u r(s)ds} f(u)\varphi\left(d^-(x, H, t, u)\right) \frac{\sigma^2(u)H}{\sqrt{\int_t^u \sigma^2(s)ds}} du \tag{3.2}$$

for $t \in [0, T)$ and $x > 0$, where $V_e(t, x)$ is the price of the standard European call on X:

$$V_e(t, x) = xe^{-\int_t^T q(s)ds}\Phi\left(d^+(x, K, t, T)\right) - Ke^{-\int_t^T r(s)ds}\Phi\left(d^-(x, K, t, T)\right) \tag{3.3}$$

with

$$d^{\pm}(x, K, t, T) = \frac{1}{\sqrt{\int_t^T \sigma^2(s)ds}}\left(\log\frac{x}{K} + \int_t^T \left(r(s) - q(s) \pm \frac{\sigma^2(s)}{2}\right)ds\right). \tag{3.4}$$

*This process is sometimes called an inhomogeneous GBM in the literature.

Remark 3.2. *The expressions presented in the theorem above, and which will be considered later, typically contain integrals of the form* $\int_t^u z(s)ds$. *To compute them, we again use the trapezoidal quadrature formula with the uniform grid* $\{t_i\}_{i=0}^m$ *already mentioned:*

$$\int_{t_i}^{t_j} z(s)ds \approx h\left(\frac{z(t_i)+z(t_j)}{2}+\sum_{k=i+1}^{j-1} z(t_k)\right). \tag{3.5}$$

As in the previous section, the pricing formula (3.2) for V involves an unknown delta $f(t)$ of V at $x = H+$. The following theorem provides a theoretical characterization of $f(t)$ and a prescription for an efficient numerical algorithm to compute it.

Theorem 3.3. *The function* $f(t)$ *satisfies the VIE of the first kind:*

$$V_e(t,H)=\frac{1}{2}\int_t^T e^{-\int_t^u r(s)ds} f(u)\varphi\left(\frac{\int_t^u\left(r(s)-q(s)-\frac{1}{2}\sigma^2(s)\right)ds}{\sqrt{\int_t^u\sigma^2(s)ds}}\right)\frac{\sigma^2(u)H}{\sqrt{\int_t^u\sigma^2(s)ds}}du \tag{3.6}$$

for $t\in[0,T)$ *with* $f(T-):=\lim_{t\uparrow T} f(t)=0$.

As in the case of constant volatility, we have a Volterra equation with a weak but integrable singularity. It is straightforward to arrive at an equation of the form (2.15) with a weak singularity by rewriting $\sqrt{\int_t^u\sigma^2(s)ds}=\sqrt{u-t}\sqrt{\frac{1}{u-t}\int_t^u\sigma^2(s)ds}$. The second term is continuous and equals $\sigma(t)$ at $u = t$ by L'Hôpital's rule. We then assume that the time-dependent parameters $r(t), q(t), \sigma(t)$ satisfy certain additional smoothness conditions. Hence, we can refer to the previous section to derive theoretical results on the Volterra integral Eq (3.6) and the numerical scheme to solve it. Once $f(t)$ is recovered numerically, we can employ the formula (3.2) to price the barrier option when X follows a geometric Brownian motion with time-dependent parameters. Figure 2 shows the behaviors of the single barrier call price and delta with respect to time for a periodic volatility function.

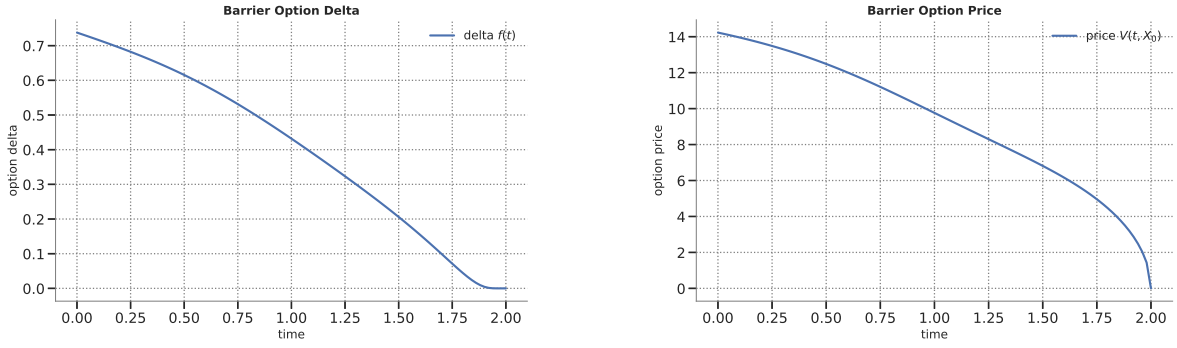

(a) single barrier option delta **(b)** single barrier option price

Figure 2. This figure displays the option's delta $f(t)$ (panel (a)) given as the solution to equation (3.6), and the single barrier option price $V(t, X_0)$ (panel (b)) computed using (3.2), both as functions of $t\in[0,T]$, where X satisfies (3.1) with time-dependent volatility. The parameters are $r = 0.05$, $\delta = 0.02$, $\sigma(t) = 0.25 + 0.05\sin(2\pi t/T)$, $T = 2$, $X_0 = 100$, $K = 100$, $H = 80$.

4. Single barrier options: stochastic volatility

In this section, we consider a general one-factor stochastic volatility model for X:

$$dX_t = (r(t) - q(t))X_t dt + \sigma_t X_t dW_t \tag{4.1}$$

$$dY_t = \alpha(t, Y_t) + \beta(t, Y_t)dZ_t \tag{4.2}$$

where $r(t)$ is the time-dependent risk-free rate, $q(t)$ is the time-dependent convenience yield, $\sigma_t = \gamma(Y_t)$ is the stochastic volatility given as a function γ of the factor process Y, and α, β are coefficients of Y that satisfy standard regularity conditions. The process Z is a Q-SBM that is correlated with W, i.e.,

$$dW = \rho(t)dZ + \sqrt{1 - \rho^2(t)}dW^{\perp} \tag{4.3}$$

where $\rho(t) \in [-1, 1]$ is the time-dependent correlation coefficient and $W^{\perp}$ is a Q-SBM that is independent of W. The SBM Z represents volatility risk. The orthogonal component $W^{\perp}$ is pure stock price risk. Volatility risk has a spillover effect on the stock price when correlation differs from zero. The case $\gamma\beta\rho < 0$ captures the leverage effect in equities documented in the literature.

We now apply the conditional Monte-Carlo method to price the down-and-out call option on X, in the spirit of [31, 33, 44]. For this, we simulate N trajectories of Z_t and hence of σ_t using, e.g., a Euler scheme with m steps. We denote them by $Z_t^{(n)}$ and $\sigma_t^{(n)}$, respectively, for $n = 1, \ldots, N$. Then, conditional on each n, we can write the dynamics of $X^{(n)}$ as

$$dX_t^{(n)} = \left(r(t) - q(t) + \rho(t)\sigma_t^{(n)}\mu_t^{(n)}\right)X_t^{(n)}dt + \sigma_t^{(n)}\sqrt{1 - \rho^2(t)}X_t^{(n)}dW_t^{\perp} \tag{4.4}$$

for $n = 1, \ldots, N$, where $\mu_t^{(n)} = \frac{dZ_t^{(n)}}{dt} - \frac{1}{2}\rho(t)\sigma_t^{(n)}$ according to [33].

Now we fix n and define $\tilde{q}^{(n)}(t) = q(t) - \rho(t)\sigma_t^{(n)}\mu_t^{(n)}$ and $\tilde{\sigma}^{(n)}(t) = \sigma_t^{(n)}\sqrt{1 - \rho^2(t)}$. Hence, we can apply the pricing method from the previous section to compute the conditional barrier option price in the model with time-dependent parameters. Figure 3 illustrates the approach for a given trajectory under the Heston stochastic volatility model. Then, the price of the barrier option can be estimated as

$$V_{SV} \approx \frac{1}{N}\sum_{n=1}^{N} V(t, x; r, \tilde{q}^{(n)}, \tilde{\sigma}^{(n)}) \tag{4.5}$$

where $V(t, x; r, \tilde{q}^{(n)}, \tilde{\sigma}^{(n)})$ is computed by the formula (3.2) for deterministic time-dependent parameters $(r, \tilde{q}^{(n)}, \tilde{\sigma}^{(n)})$. The definition of $\tilde{q}^{(n)}(t)$ may appear to be confusing, since it includes the term $\frac{dZ_t^{(n)}}{dt}$, even though Brownian motion is nowhere differentiable. This should be interpreted as a formal expression. Fortunately, the dividend yield $\tilde{q}^{(n)}(t)$ in all formulas above and below appears under the integral sign. Thus, substituting $\tilde{q}^{(n)}(t)$ in the integral gives

$$\int_t^u \tilde{q}^{(n)}(s)ds = \int_t^u q(s)ds - \int_t^u \rho(s)\sigma_s^{(n)}dZ_s^{(n)} + \frac{1}{2}\int_t^u \rho^2(s)(\sigma_s^{(n)})^2 ds \tag{4.6}$$

where the second term is a stochastic integral, which is computed numerically as the sum $\sum_{k=i}^{j-1}\rho(t_k)\sigma_{t_k}^{(n)}(Z_{t_{k+1}}^{(n)} - Z_{t_k}^{(n)})$ over a uniform grid $t = t_i < \ldots < t_j = u$.

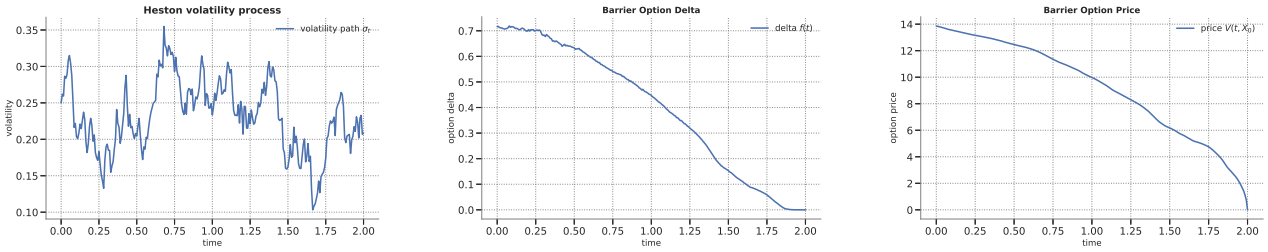

(a) trajectory of volatility **(b)** barrier option delta **(c)** single barrier option price

Figure 3. This figure displays the option's delta $f(t)$ (panel (b)) given as the solution to the Eq (3.6), and the single barrier option price $V(t, X_0)$ (panel (c)) computed using (3.2), both as functions of $t \in [0, T]$, where X satisfies (3.1) with time-dependent volatility. The latter was generated by a single trajectory σ_t (panel (a)) under the Heston model $d\sigma_t^2 = \kappa(\theta - \sigma_t^2)dt + \eta\sigma_t dZ_t$, and the correlation between Z and W is given by a constant parameter $\rho = 0$. The parameters are $r = 0.05$, $\delta = 0.02$, $\sigma_0 = 0.25$, $\kappa = 2$, $\theta = 0.09$, $\eta = 0.4$, $T = 2$, $X_0 = 100$, $K = 100$, $H = 80$.

To achieve higher accuracy, we follow [44] and use the quasi-Monte Carlo method. Low-discrepancy sequences (e.g., Sobol or Halton) are employed to simulate the Brownian driver Z of the stochastic volatility process. We choose the number of time steps as $m = 2^I$ for some integer I. The m-dimensional vector $\mathbf{x}^n$ is drawn from a low-discrepancy sequence uniformly distributed over $[0, 1]^m$ for $n = 1, \ldots, N$, and its component $\mathbf{x}_j^n$ transformed via $\Phi^{-1}(\mathbf{x}_j^n)$, where Φ^{-1} is the inverse function of the cumulative distribution function of the standard normal law. The Brownian paths Z are generated using the Brownian bridge construction via binary midpoint refinement as in [6]. We fix the endpoints as $Z_0^{(n)} = 0$ and $Z_T^{(n)} = \sqrt{T}\Phi^{-1}(\mathbf{x}_m^n)$. Then, recursively, at each level $i = 1, \ldots, I$, we halve the step size $h \to h/2$, and for each midpoint $(2j-1)h$, we set

$$Z_{(2j-1)h}^{(n)} = \frac{1}{2}(Z_{2(j-1)h}^{(n)} + Z_{2jh}^{(n)}) + \sqrt{\frac{h}{2}}\Phi^{-1}\left(\mathbf{x}_{(2j-1)h}^n\right), \quad j = 1, \ldots, 2^{i-1}. \tag{4.7}$$

This method, in combination with quasi-Monte Carlo sampling, produces a path of length m and offers improved convergence properties.

5. Double barrier options: stochastic volatility

In this section, we turn to the pricing of double barrier options with a knock-out feature and zero rebate. Let us assume the strike K, two barriers $H_1 < K < H_2$, and the maturity date T. The price of the double barrier option $V(t, x)$ can be defined as

$$V(t, x) = \mathbb{E}_{t,x}\left[e^{-\int_t^T r(s)ds}(X_T - K)^+ I(M_T < H_2, m_T > H_1)|H_1 < m_t \le M_t < H_2\right] \tag{5.1}$$

for $t \in [0, T)$ and $H_1 < x < H_2$, where the expectation is taken under Q, and the elements of the pair (M_T, m_T) represent the maximum and the minimum of the underlying asset price:

$$M_T = \max_{0\le t\le T} X_t, \quad m_T = \min_{0\le t\le T} X_t. \tag{5.2}$$

We first assume that the risk-neutral dynamics of X are given by (3.1) with time-dependent parameters. The fixed boundary PDE system for V can be formulated as follows:

$$\frac{\partial}{\partial t}V + \mathbb{L}V = r(t)V, \quad t \in [0,T), \quad H_1 < x < H_2, \tag{5.3}$$

$$V(t,x) = 0, \quad t \in [0,T), \quad x \le H_1 \text{ or } x \ge H_2, \tag{5.4}$$

$$V(T,x) = (x-K)^+ I(x < H_2), \quad x > 0, \tag{5.5}$$

where the operator of $\mathbb{L}$ of X is given by

$$\mathbb{L}f(t,x) = (r(t) - q(t))xf_x(t,x) + \frac{1}{2}\sigma^2(t)x^2 f_{xx}(t,x) \tag{5.6}$$

for $f \in C^{1,2}$. Using the local time-space approach, we derive the double barrier option price and obtain the following result.

Theorem 5.1. *The double barrier option price* (5.1) *can be decomposed as*

$$\begin{aligned} V(t,x) =& V_0(t,x) - \frac{1}{2}\int_t^T e^{-\int_t^u r(s)ds} f_1(u)\varphi\left(d^-(x,H_1,t,u)\right)\frac{\sigma^2(u)H_1}{\sqrt{\int_t^u \sigma^2(s)ds}}du \\ &+ \frac{1}{2}\int_t^T e^{-\int_t^u r(s)ds} f_2(u)\varphi\left(d^-(x,H_2,t,u)\right)\frac{\sigma^2(u)H_2}{\sqrt{\int_t^u \sigma^2(s)ds}}du \end{aligned} \tag{5.7}$$

for $t \in [0,T)$ and $x > 0$, where $f_1(t) := V_x(t,H_1+)$ and $f_2(t) := V_x(t,H_2-)$, and V_0 is the price of the European-style derivative with payoff $(X_T - K)^+ I(X_T < H_2)$

$$\begin{aligned} V_0(t,x) =& \mathbb{E}_{t,x}[e^{-\int_t^T r(s)ds}(X_T - K)^+ I(X_T < H_2)] \\ =& \mathbb{E}_{t,x}[e^{-\int_t^T r(s)ds} X_T I(K < X_T < H_2)] - \mathbb{E}_{t,x}[e^{-\int_t^T r(s)ds} K I(K < X_T < H_2)] \\ =& xe^{-\int_t^T q(s)ds}(\Phi\left(d^+(x,K,t,T)\right) - \Phi\left(d^+(x,H_2,t,T)\right)) \\ & - Ke^{-\int_t^T r(s)ds}\left(\Phi\left(d^-(x,K,t,T)\right) - \Phi\left(d^-(x,H_2,t,T)\right)\right) \end{aligned} \tag{5.8}$$

and $d^\pm$ was given in (3.4)*.*

A sketch of the proof is provided in the Appendix. The pricing formula above involves (yet) unknown functions $f_1(t)$ and $f_2(t)$ that are the barrier option's deltas at $x = H_1+$ and $x = H_2-$, respectively, for $t \in [0,T)$. The next result characterizes them.

Theorem 5.2. *The functions $f_1(t)$, $f_2(t)$ are the solution of the following system of coupled linear Volterra integral equations of the first kind:*

$$\begin{aligned} V_0(t,H_1) =& \frac{1}{2}\int_t^T e^{-\int_t^u r(s)ds} f_1(u)\varphi\left(d^-(H_1,H_1,t,u)\right)\frac{\sigma^2(u)H_1}{\sqrt{\int_t^u \sigma^2(s)ds}}du \\ & - \frac{1}{2}\int_t^T e^{-\int_t^u r(s)ds} f_2(u)\varphi\left(d^-(H_1,H_2,t,u)\right)\frac{\sigma^2(u)H_2}{\sqrt{\int_t^u \sigma^2(s)ds}}du; \end{aligned} \tag{5.9}$$

$$V_0(t,H_2) = \frac{1}{2}\int_t^T e^{-\int_t^u r(s)ds} f_1(u)\varphi\left(d^-(H_2,H_1,t,u)\right)\frac{\sigma^2(u)H_1}{\sqrt{\int_t^u \sigma^2(s)ds}}du \tag{5.10}$$
$$-\frac{1}{2}\int_t^T e^{-\int_t^u r(s)ds} f_2(u)\varphi\left(d^-(H_2,H_2,t,u)\right)\frac{\sigma^2(u)H_2}{\sqrt{\int_t^u \sigma^2(s)ds}}du$$

for $t \in [0,T)$, where V_0 is the price of the European-style derivative from Theorem 5.1.

As in the one-dimensional case, we provide conditions for the existence and uniqueness of a solution to this system. To begin with, we introduce a special case of a weighted Sobolev space, as in [26]. Let $T > 0$; $n, m \in \mathbb{N}$; and $\gamma < 1$. Define $C^n_\gamma[0,T] := \{F : [0,T] \to \mathbb{R}^m \,|\, t^\gamma F(t) \in C^n[0,T]\}$, with intrinsic norm

$$\|F\|_{\gamma,n} := \sum_{k=0}^{n} \sup_{0\le t\le T} \left\| \frac{d^k}{dt^k}\left(t^\gamma F(t)\right)\right\|, \tag{5.11}$$

where $\|\cdot\|$ is some vector norm. The map $\mathcal{J}_\gamma : C^n_\gamma[0,T] \to C^n[0,T]$, $\mathcal{J}_\gamma(F)(t) = t^\gamma F(t)$, is a linear isometric isomorphism. Hence $C^n_\gamma[0,T]$ is a separable Banach space. After that, we appeal to the following generalization for systems of equations from [2]:

Theorem 5.3. *Consider the Abel-type equation system:*

$$G(t) = \int_0^t \frac{F(u)K(t,u)}{(t-u)^\alpha}du, \quad 0 < t \le T, \tag{5.12}$$

with $\alpha \in (0,1)$, vector functions $F, G : [0,T] \to \mathbb{R}^m$, $F(t) = [f_1(t),\dots,f_m(t)]^T$, $G(t) = [g_1(t),\dots,g_m(t)]^T$, and the matrix kernel $K : [0,T]^2 \to \mathbb{R}^{m\times m}$, $K(t,s) = \left[k_{ij}(t,s)\right]_{i,j=1}^m$. Assume that

(a) $G(t) = t^{-\beta}G_0(t)$ with $G_0 \in C^{n+1}[0,T]$ for some $n \in \mathbb{N}$ and $\alpha > \beta$;
(b) $K(\cdot,\cdot)$ is sufficiently smooth on $0 \le t \le s \le T$ (as in the scalar Atkinson theorem, up to the order needed for the estimates below);
(c) $\det K(t,t) \neq 0$ for every $t \in [0,T]$.

Then:

(1) There exists a unique solution F of the form

$$F(t) = t^{\alpha-\beta-1}[B + tF_0(t)], \quad F_0 \in C^n[0,T], \quad B \in \mathbb{R}^m. \tag{5.13}$$

Equivalently, $F \in C^n_{1-\alpha+\beta}[0,T]$ and $\lim_{t\downarrow 0} t^{1-\alpha+\beta}F(t) = B$.
(2) There is a constant $C > 0$, independent of $G(t)$, such that the unique solution satisfies

$$\|F\|_{1-\alpha+\beta,n} \le C\|G\|_{\beta,n+1}. \tag{5.14}$$

As stated in the original work of [2], the proof from the one-dimensional setting can be carried over by simply replacing absolute values with suitable vector and matrix norms. Alternatively, one may extend the result by applying the method in [42] combined with Theorem 5.4 of [29].

It remains to verify the validity of the theorem for our case. We have a two-dimensional system with $\alpha = 1/2$, where the left-hand side is $G = [g_1, g_2]$ and the kernel is a 2×2 matrix $K = [\tilde{k}_{ij}]_{i,j=1}^2$, defined in the equations below. We seek a solution of the form $F(t) = [f_1(T-t), f_2(T-t)]$. The smoothness order of the data K and G depends directly on the coefficients r, q, and σ. For constant coefficients, these functions are analytic. Because $g_1(0) = V_0(T, H_1) = 0$ and $g_2(0) = V_0(T, H_2) = (H_2 - K)/2 > 0$, it follows that $\beta = 0$. Moreover, the matrix $K(t,t)$ is invertible, since $\tilde{k}_{12}(t,t) = \tilde{k}_{21}(t,t) = 0$ for $0 \le t \le T$, and

$$\tilde{k}_{ii}(t,t) = \frac{\sigma(t) H_i}{2\sqrt{2\pi}} > 0, i = 1, 2.$$

Thus, the solution F belongs to the weighted Sobolev space $C^n_{1/2}$ and the problem is well-posed.

Remark 5.4. *It can be seen that, as for the up-and-out call option, the delta f_2 of the double barrier option at the upper barrier explodes to $-\infty$ as t approaches T. Below we describe how to handle this issue numerically.*

To regularize the function $f_2(t)$, we introduce the transformed function $\bar{f}_2(t) = (T-t)^\lambda f_2(t)$ for some $1/2 \le \lambda < 1$, ensuring it remains bounded at T. For the case $\lambda = 1/2$, we have $\bar{f}_2(T-) = B > 0$; whereas for $\lambda \in (1/2, 1)$, we obtain $\bar{f}_2(T-) = 0$. The modified system can be treated by the product integration method. Using a change of variables, the system is easily rewritten in the following general form:

$$g_1(t) = \int_0^t \frac{\tilde{f}_1(u)\tilde{k}_{11}(t,u)}{\sqrt{t-u}} du - \int_0^t \frac{\tilde{f}_2(u)\tilde{k}_{12}(t,u)}{u^\lambda \sqrt{t-u}} du, \tag{5.15}$$

$$g_2(t) = \int_0^t \frac{\tilde{f}_1(u)\tilde{k}_{21}(t,u)}{\sqrt{t-u}} du - \int_0^t \frac{\tilde{f}_2(u)\tilde{k}_{22}(t,u)}{u^\lambda \sqrt{t-u}} du, \tag{5.16}$$

where $g_p(t) = V_0(T-t, H_p)$, $\tilde{f}_1(t) = f_1(T-t)$, $\tilde{f}_2(t) = \bar{f}_2(T-t)$, and $\tilde{k}_{lp}(t,s)$ are the kernels determined from Theorem 5.2 for $l, p = 1, 2$. As before, we use a uniform time grid $\{t_i\}_{i=0}^m$. The functions with superscripts i, j without arguments represent their discrete values at the corresponding grid points t_i or t_j. The approximate solutions on the given grid are denoted by $\hat{f}_1^j$ and $\hat{f}_2^j$. For simplicity, set $\lambda = 1/2$ and replace the integrands $\tilde{f}_p(u)\tilde{k}_{lp}(t,u)$ by the rightpoint piecewise constant functions

$$\tilde{k}_{lp}^{i,j+1} \hat{f}_p^{j+1}, \quad t_j < u \le t_{j+1}, \quad j = 0, 1, \ldots, i-1. \tag{5.17}$$

This yields the following block form triangular system for the approximations $\hat{f}_1^j$ and $\hat{f}_2^j$:

$$\begin{cases} \sum_{j=1}^i \hat{f}_1^j \tilde{k}_{11}^{i,j} \omega_{i,j}^1 + \sum_{j=1}^i \hat{f}_2^j \tilde{k}_{12}^{i,j} \omega_{i,j}^2 = g_1^i \\ \sum_{j=1}^i \hat{f}_1^j \tilde{k}_{21}^{i,j} \omega_{i,j}^1 + \sum_{j=1}^i \hat{f}_2^j \tilde{k}_{22}^{i,j} \omega_{i,j}^2 = g_2^i \end{cases} \quad i = 1, \ldots, m, \tag{5.18}$$

where $\omega_{i,j}^1$ and $\omega_{i,j}^2$ are precomputed weights:

$$\omega_{i,j}^1 = 2\Delta t^{1/2} \left(\sqrt{i-j+1} - \sqrt{i-j} \right), \tag{5.19}$$

$$\omega_{i,j}^2 = 2 \left(\arcsin(\sqrt{j/i}) - \arcsin(\sqrt{(j-1)/i}) \right) \tag{5.20}$$

for $j \leq i$. The result can be expressed in a compact matrix form as

$$\begin{pmatrix} g_1 \\ g_2 \end{pmatrix} = \begin{pmatrix} A_{11} & A_{12} \\ A_{21} & A_{22} \end{pmatrix} \begin{pmatrix} \hat{f}_1 \\ \hat{f}_2 \end{pmatrix} \tag{5.21}$$

where

$$g_p = \left(g_p^1, \ldots, g_p^m\right)^T, \hat{f}_p = \left(\hat{f}_p^1, \ldots, \hat{f}_p^m\right)^T$$

are vectors and A_{lp}, $l, p = 1, 2$, are lower triangular matrices. Once the option deltas $f_1(t)$, $f_2(t)$ are computed numerically, the double barrier option price $V(t, x)$ can be easily obtained, similarly to the single barrier case, using (5.7) and applying quadrature rules.

With the characterization of the price of the double barrier option under time-dependent GBM (3.1), we can now price it under the stochastic volatility models (4.1) and (4.2). For this, we adopt the same argument with outer and inner loops as in Section 4, i.e., Eq (4.5).

6. Numerical study

6.1. Models and parameters

We now conduct a numerical study to illustrate the behaviors of barrier option prices and deltas. Three models for the underlying price evolution are considered: geometric Brownian motion (GBM), GBM with time-dependent volatility (GBM-TDV), and conditional geometric Brownian motion with mean reverting square root volatility process (CGBM-MRSRV), as proposed by [19]. Benchmark parameter values for the different models examined are listed in Table 2. All options considered are at-the-money (ATM) call options with $T = 2, X_0 = 100, K = 100$. Single barrier options have $H = 80$. Double barrier options have $H_1 = 70, H_2 = 130$. Deltas are calculated at the barriers. Option Greeks mentioned in the discussions below are defined in Table 3. It is understood that the properties of prices, deltas and other Greeks that are documented in our numerical experiments may be parameter-specific, i.e., there is no claim of generality.

Table 2. Price models and parameters. Models are geometric Brownian motion (GBM), geometric Brownian motion with time-dependent volatility (GBM-TDV), and conditional geometric Brownian motion with mean reverting square root volatility (CGBM-MRSRV) as in [19]. Parameter σ_0 is the initial volatility. Cumulative ex-dividend return R_t satisfies $dR_t = dS_t/S_t$.

Parameter	**GBM**	**GBM-TDV**	**CGBM-MRSRV**
	$dR_t = (r-q)dt + \sigma dW_t$	$dR_t = (r-q)dt + \sigma_t dW_t$ $\sigma_t = \sigma_0 + \omega \sin(2\pi t/T)$	$dR_t = (r-q)dt + \sigma_t dW_t$ $d\sigma_t^2 = \kappa(\theta - \sigma_t^2)dt + \eta\sigma_t dZ_t$
r	0.05	0.05	0.05
δ	0.02	0.02	0.02
σ_0	0.30	0.25	0.25
ω	–	0.05	–
κ	–	–	2
θ	–	–	0.09
η	–	–	$\{0.25, 0.4\}$
ρ	–	–	0

Table 3. Option Greeks. Option Greeks in the one-factor stochastic volatility models (4.1) and (4.2) with $Y = \sigma$. The price function is $V(t, x, \sigma; \tau)$ where τ is the time-to-maturity. There is no standard letter notation for charm, vanna, and vomma.

Greek	Formula
Delta	$\Delta(t, x, \sigma; \tau) = \frac{\partial V(t,x,\sigma;\tau)}{\partial x}$
Theta	$\Theta(t, x, \sigma; \tau) = -\frac{\partial V(t,x,\sigma;\tau)}{\partial \tau}$
Vega	$\mathcal{V}(t, x, \sigma; \tau) = \frac{\partial V(t,x,\sigma;\tau)}{\partial \sigma}$
Charm	$\text{Charm}(t, x, \sigma; \tau) = -\frac{\partial \Delta(t,x,\sigma;\tau)}{\partial \tau}$
Vanna	$\text{Vanna}(t, x, \sigma; \tau) = \frac{\partial \Delta(t,x,\sigma;\tau)}{\partial \sigma}$
Vomma	$\text{Vomma}(t, x, \sigma; \tau) = \frac{\partial \mathcal{V}(t,x,\sigma;\tau)}{\partial \sigma}$

6.2. Numerical scheme: convergence

We first examine the convergence properties of the numerical algorithm. Table 4 provides results for the double barrier option price as m increases, in the model with constant volatility. It shows convergence is fast over the range of maturity dates examined.

Table 4. This table shows the convergence of the double barrier knock-out option price based on the representation (5.7) to the exact price given in [37], in the case of constant volatility, as a function of the number of time steps m in the numerical scheme. The parameters are $r = 0.05$, $\delta = 0.02$, $\sigma = 0.3$, $X_0 = 100$, $K = 100$, $H_1 = 70$, $H_2 = 130$.

Maturity	Exact	$m = 16$	$m = 64$	$m = 128$	$m = 256$
0.125	4.0174	4.0220	4.0181	4.0177	4.0175
0.25	4.0069	4.0236	4.0095	4.0079	4.0073
0.5	2.8013	2.8311	2.8060	2.8032	2.8021
1.0	1.4004	1.4331	1.4057	1.4025	1.4012
1.5	0.7508	0.7745	0.7544	0.7521	0.7513

To assess the scheme's performance when volatility is stochastic, we consider the Heston CGBM-MRSRV model with parameters given in Table 2. To measure accuracy, we use the well-known relative root mean square error (RMSE) metric, which is sensitive to outliers and captures large errors. As a benchmark price, we make use of the program obtained from [41] based of the finite difference method with a sufficiently large grid $(1000, 1000, 1000)$ in time, stock price, and volatility. For the RMSE computation for our method, we employ a scrambled Sobol' sequence; see for instance [10]. We fix the number of time steps at $m = 64$ and $m = 128$ for single and double barrier options, respectively. Then, for a given number N of sequences, we obtain option prices and compute the corresponding RMSE by repeating the price calculations for 32 independent realizations (scrambles) of the Sobol' sequences. The results are reported in Table 5 for the single barrier call option and in Table 6 for the double barrier one.[†] For comparison, we also provide RMSE values obtained using plain Monte Carlo (MC). MC prices are calculated using $2^n, n = 12, 14, 16$ trajectories with a time discretization grid of

[†]All numerical experiments were performed in the cloud environment Google Colaboratory (Python 3.12) without using GPU or TPU accelerators. The computations were carried out on a virtual machine equipped with an Intel(R) Xeon(R) CPU @ 2.20GHz (2 cores, 4 threads) and 12 GB of RAM. The elapsing time for our scheme for a single barrier option with $N = 512$ was 1.92 seconds, while for a double barrier option with $N = 512$ it was 8.53 seconds.

size 1024. RMSE is calculated by repeating these computations using 64 different seeds (samples) of the random number generator. As can be seen from the table, the convergence rate for our method is approximately $O(1/N)$, whereas for Monte Carlo it is only $O(1/\sqrt{N})$.

Table 5. This table presents the relative RMSE (in %) of the down-and-out barrier option price based on the representation (4.5) (with N trajectories) and standard Monte Carlo (with 2^n trajectories), compared to the benchmark price obtained via the finite difference method in QuantLib, under the Heston model. The model parameters are provided in the Table 2 ($\eta = 0.4$) with fixed $T = 1$, $X_0 = 100$, and $H = 80$.

ρ	K	**Benchmark**	**Our Approach**			**Plain MC**		
			$N = 128$	$N = 256$	$N = 512$	$n = 12$	$n = 14$	$n = 16$
−0.5	110	**7.2238**	0.53	0.38	0.17	3.27	1.91	0.84
−0.5	100	**11.1267**	0.52	0.37	0.15	2.38	1.14	0.97
−0.5	90	**15.9777**	0.47	0.31	0.15	2.37	1.44	0.90
0.0	110	**7.6310**	0.16	0.07	0.05	3.34	1.82	1.09
0.0	100	**11.2548**	0.09	0.06	0.03	3.15	1.55	0.98
0.0	90	**15.9616**	0.04	0.02	0.01	2.40	1.19	0.81

Table 6. This table presents the relative RMSE (in %) of the double knock-out barrier option price based on the representation (4.5) (with N trajectories) and standard Monte Carlo (with 2^n trajectories), compared to the benchmark price obtained via the finite difference method in QuantLib, under the Heston model. The model parameters are provided in Table 2 ($\eta = 0.4$) with fixed $T = 1$, $X_0 = 100$ and barriers $H_1 = 70$, $H_2 = 130$.

ρ	K	**Benchmark**	**Our Approach**			**Plain MC**		
			$N = 128$	$N = 256$	$N = 512$	$n = 12$	$n = 14$	$n = 16$
−0.5	110	**0.8457**	1.98	1.38	0.78	2.66	1.32	0.80
−0.5	100	**2.5663**	1.34	0.79	0.54	3.27	2.13	0.92
−0.5	90	**5.4190**	1.51	0.97	0.52	5.88	2.48	1.48
0.0	110	**0.5673**	0.42	0.24	0.14	2.92	1.49	0.60
0.0	100	**1.9188**	0.39	0.18	0.13	3.72	2.13	1.00
0.0	90	**4.4298**	0.43	0.17	0.10	7.00	3.00	1.54

6.3. Numerical results

Figure 1 illustrates the behavior with respect to time of the delta (panel (a)) and price (panel (b)) of a (single barrier) down-and-out call option in the Black-Scholes setting. Since the option considered is ATM ($X_0 = K$), the price converges to zero as the maturity date approaches and the option's theta (its time decay), which is negative throughout, goes to negative infinity. The pattern displayed reflects the fact that $K > H$. Delta is evaluated at the barrier $X_0 = H$. It decreases quickly when the time-to-maturity is sufficiently long, but the negative delta time decay, i.e., the option's charm, eventually increases and converges to zero. Figure 2, which considers the case of a sinusoidal time-dependent volatility, displays the same broad patterns. In this instance, the option's theta and charm slow down

or accelerate at times, reflecting the additional effects of variations in volatility. Figure 3 shows the impact of stochastic volatility in the Heston model. Delta (panel (b)) and price (panel (c)) are displayed conditional on a realized trajectory of volatility (panel (a)), assuming null correlation. General patterns are again similar to those recorded in the previous two models. In this case, however, the option delta, its price, and their respective time decays exhibit more erratic variations reflecting the additional effects of the variations in realized volatility.

The behavior of double barrier knock-out options is displayed in Figures 4–9. Figure 4 shows that the ATM call price in the GBM model steadily increases as time progresses before collapsing to zero close to maturity. This behavior reflects two conflicting forces. On the one hand, the likelihood of hitting the knock-out barriers prior to maturity decreases as time-to-maturity shrinks. On the other hand, the likelihood of a significant increase in the underlying price above the strike decreases. The first effect ensures the price increases since the likelihood of ending up in-the-money increases. The second effect reduces the price since the upside potential decreases. The first (second) effect dominates far from (close to) maturity, leading to the behavior displayed. The behavior of the delta at the lower barrier reflects the price behavior, except close to the maturity date where the associated charm converges to zero, as in previous models. The delta at the upper barrier is negative because the option price converges to zero when the underlying price approaches the upper barrier. It decreases over time, initially slowly, then quickly when the maturity date approaches. Its charm is negative throughout and converges to negative infinity at maturity. The pattern reflects the behavior of the likelihood of early knock-out as the maturity date approaches.

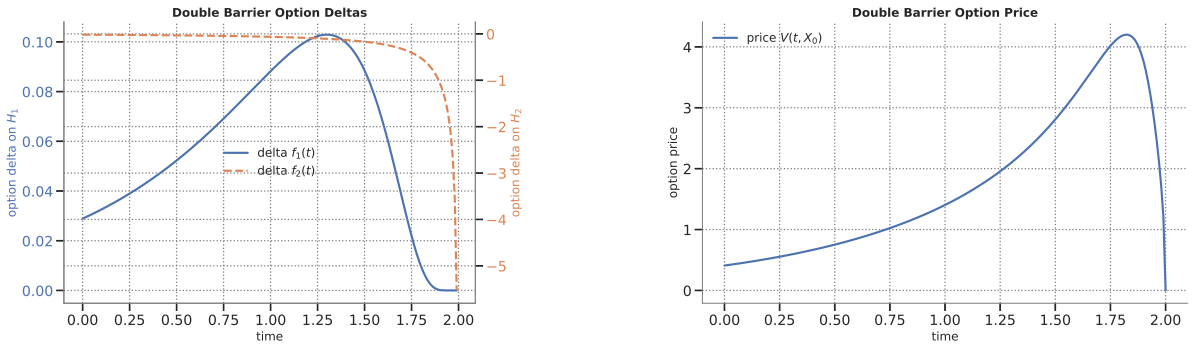

(a) double barrier option delta **(b)** double barrier option price

Figure 4. This figure displays the option's deltas $f_1(t)$ and $f_2(t)$ (panel (a)) given as the solutions to the system of Eqs (5.9) and (5.10), and the double barrier knock-out option price $V(t, X_0)$ (panel (b)) computed using (5.7), all as functions of $t \in [0, T]$, in the GBM model. The parameters are $r = 0.05$, $\delta = 0.02$, $\sigma = 0.3$, $T = 2$, $X_0 = 100$, $K = 100$, $H_1 = 70$, $H_2 = 130$. The scale for f_1 on the left side is positive. The scale for f_2 on the right side is negative.

Figures 5–9 compare the behaviors of single and double barrier knock-out call prices in the Heston model when parameters of the volatility process or the initial volatility level change. All cases reveal significant differences in behavior across knock-out types (single versus double). To explain the patterns recorded, it is useful to recall the behavior of option prices conditional on a volatility trajectory. For a down-and-out call, the conditional option price is convex with respect to the

underlying price, implying it increases with volatility. In contrast, the conditional price of a double barrier knock-out call has an asymmetric bell-like structure with respect to the underlying price due to the knock-outs at the lower and upper barriers. It therefore responds negatively to volatility, except perhaps in the neighborhoods of the barriers. When the speed of mean reversion increases, volatility reverts faster to its long run mean, hence it decreases faster on average in the short run given benchmark parameters, but over the long run increases along trajectory segments below the long run mean. The first effect puts downward (upward) pressure on the conditional single (double) barrier knock-out price, while the second one has the opposite impact, for each trajectory of volatility risk Z. The increased speed of reversion also implies a reduction in the likelihood of hitting the lower knock-out barrier in the short run, which enhances conditional values. Figure 5 shows that the price of a single barrier knock-out call increases in response, suggesting the negative short run effect is dominated, once the conditional price is averaged. In contrast, the price of a double barrier knock-out call decreases (increases) when time-to-maturity is long (short). In this instance, there is the additional possibility of a knock-out at the upper barrier. The short run decrease in volatility reduces the likelihood of hitting the upper barrier, and this has a positive effect on short-dated call prices. Long-dated call prices also reflect the increase in volatility along trajectory segments below the long run mean, and this effect puts downward pressure on prices.

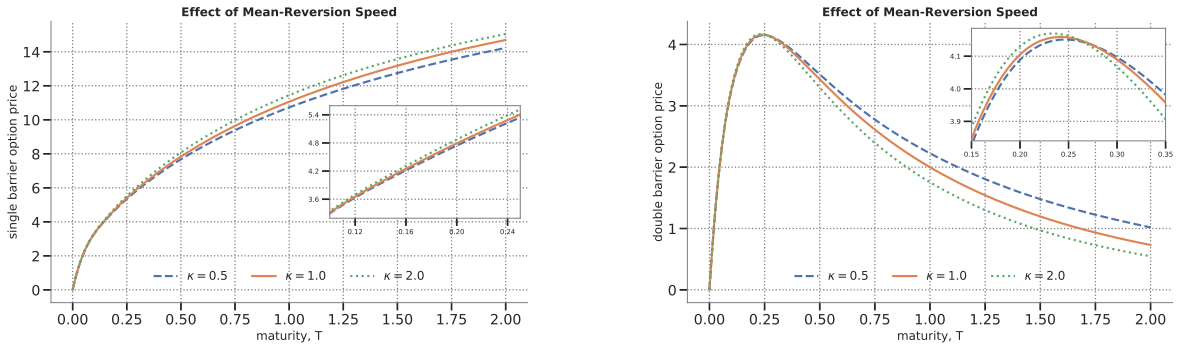

(a) single barrier option price

(b) double barrier option price

Figure 5. This figure displays the effect of the mean-reversion speed κ on the single barrier option price with $H = 80$ (panel (a)) and the double barrier option price with $H_1 = 70 < H_2 = 130$ (panel (b)) both as functions of maturity T. The inner windows magnify effects over a selected range. The dynamics of X are given by the Heston model with $\kappa = 0.5$ (dashed), $\kappa = 1$ (solid), $\kappa = 2$ (dotted). The other parameters are $r = 0.05$, $\delta = 0.02$, $\sigma_0 = 0.25$, $\theta = 0.09$, $\eta = 0.25$, $\rho = 0$, $T = 2$, $X_0 = 100$, $K = 100$.

Figure 6 displays similar differences in behavior across barrier option types when the long run mean increases. In this case, volatility increases, uniformly over time, implying the associated effects described in the previous paragraph are at play. Accordingly, the single (double) barrier knock-out call price increases (decreases far from maturity and increases close to it). Figure 7 shows the effects of the vol-of-vol parameter. Here, it is useful to note that the conditional prices of ATM single barrier and short-dated double barrier knock-out calls are concave with respect to volatility, whereas the conditional price of an ATM long-dated double barrier knock-out call is convex. An increase in vol-of-vol increases the sensitivity of volatility to innovations which raises the likelihood of extreme

volatility realizations and puts downward (upward) pressure on the price of a volatility-linked claim with concave (convex) payoff. The increased likelihood of high or low volatility bursts has the additional effect of raising the prospect of an early knock-out. Extreme volatility reinforces (tames) the concavity (convexity) effect described above. The figure shows the single barrier and short-maturity double barrier knock-out call prices decrease as a result of these conflicting effects. Panel (b) of the figure shows the positive effect dominates for long-maturity double barrier knock-out calls. Figure 8 displays the impact of the correlation between the underlying price and volatility. An increase in correlation from negative to positive ensures the two processes tend to move more consistently in the same direction. On average, a high (low) underlying price is then associated with high (low) volatility. As the likelihood of hitting a low barrier decreases, the price of the single barrier knock-out call increases. The reverse is true for the double barrier knock-out call due to the increased likelihood of hitting the upper knock-out barrier.

Lastly, Figure 9 shows the impact of initial volatility on the deltas and vegas of ATM single and double barrier knock-out calls for different time slices. Differences across barrier types are quite striking. The deltas of ATM double barrier calls with long maturities do not vary much with respect to volatility over the range examined, in contrast to ATM single barrier calls. The reverse is true for very short-dated contracts, e.g., when time-to-maturity is smaller than or equal to 0.5, where vanna can reach substantially larger negative values. Vegas, like deltas, are more sensitive to volatility at short maturities. Across barrier types, vegas of ATM double barrier options tend to vanish faster as volatility increases. They also display increasing patterns, except at very short maturities (vegas of ATM single barrier calls are mostly decreasing with respect to volatility). At those short maturities vommas are negative and can attain large values. These results therefore suggest that the implementation of effective delta hedging and vega hedging strategies will be more challenging for short-dated double barrier contracts as compared to short-dated single barrier contracts, but less challenging in other cases.

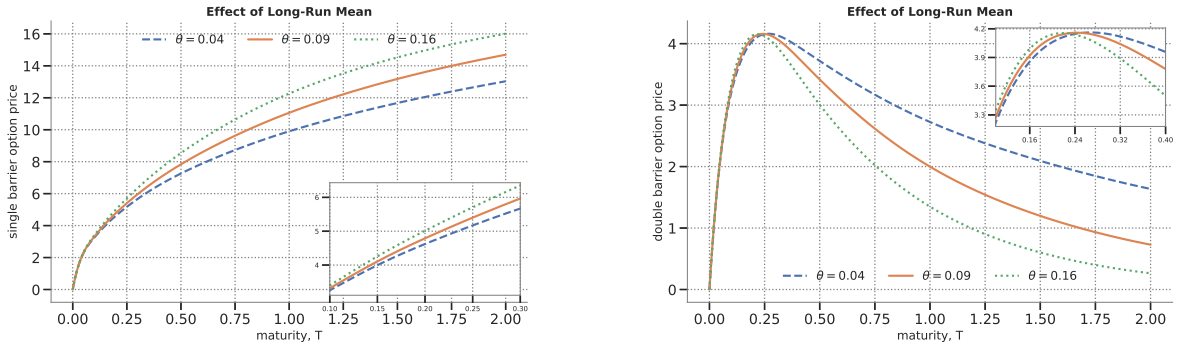

(a) single barrier option price

(b) double barrier option price

Figure 6. This figure displays the effect of the long-run mean θ on the single barrier option price with $H = 80$ (panel (a)) and the double barrier option price with $H_1 = 70 < H_2 = 130$ (panel (b)) both as functions of maturity T. The inner windows magnify the effects over a selected range. The dynamics of X are given by the Heston model with $\theta = 0.2^2$ (dashed), $\theta = 0.3^2$ (solid), $\theta = 0.4^2$ (dotted). The other parameters are $r = 0.05$, $\delta = 0.02$, $\sigma_0 = 0.25$, $\kappa = 1$, $\eta = 0.25$, $\rho = 0$, $T = 2$, $X_0 = 100$, $K = 100$.

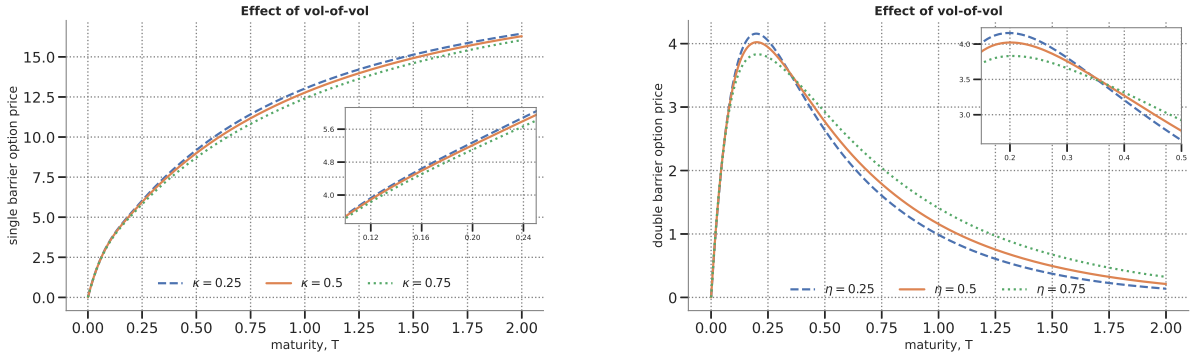

(a) single barrier option price **(b)** double barrier option price

Figure 7. This figure displays the effect of the vol-of-vol parameter η on the single barrier option price with $H = 80$ (panel (a)) and the double barrier option price with $H_1 = 70 < H_2 = 130$ (panel (b)) both as functions of maturity T. The inner windows magnify the effects over a selected range. The dynamics of X are given by the Heston model with $\eta = 0.25$ (dashed), $\eta = 0.5$ (solid), $\eta = 0.75$ (dotted). The other parameters are $r = 0.05$, $\delta = 0.02$, $\sigma_0 = 0.25$, $\kappa = 2$, $\theta = 0.16$, $\rho = 0$, $T = 2$, $X_0 = 100$, $K = 100$.

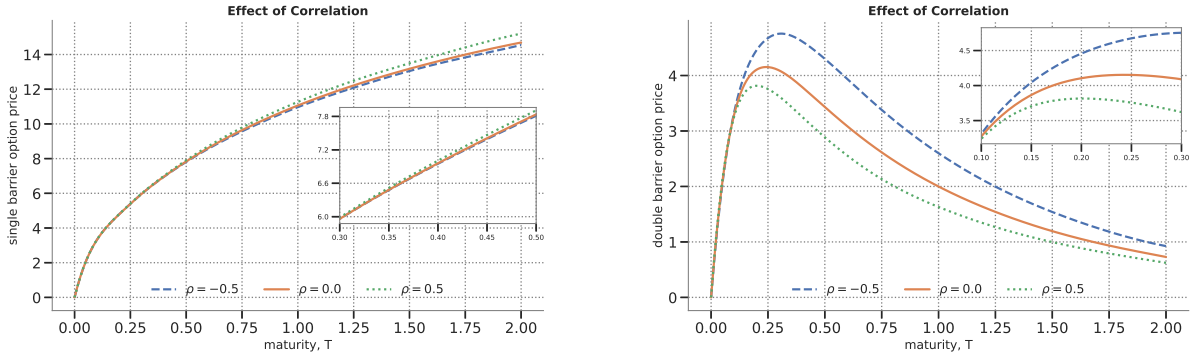

(a) single barrier option price **(b)** double barrier option price

Figure 8. This figure displays the effect of the correlation parameter ρ on the single barrier option price with $H = 80$ (panel (a)) and the double barrier option price with $H_1 = 70 < H_2 = 130$ (panel (b)) both as functions of maturity T. The inner windows magnify the effects over a selected range. The dynamics of X are given by the Heston model with $\rho = -0.5$ (dashed), $\rho = 0$ (solid), $\rho = 0.5$ (dotted). The other parameters are $r = 0.05$, $\delta = 0.02$, $\sigma_0 = 0.25$, $\kappa = 1$, $\theta = 0.09$, $\eta = 0.25$, $T = 2$, $X_0 = 100$, $K = 100$.

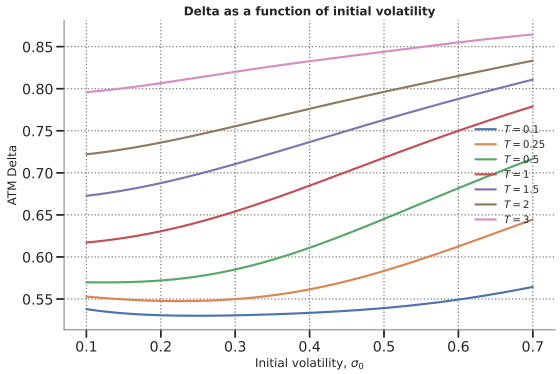

(a) Delta of single barrier option

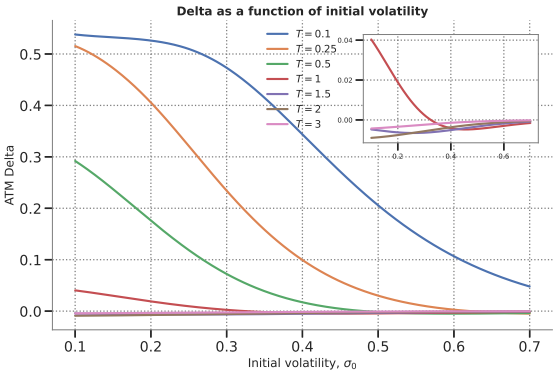

(b) Delta of double barrier option

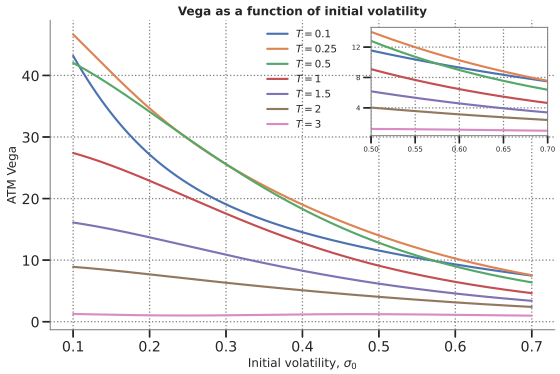

(c) Vega of single barrier option

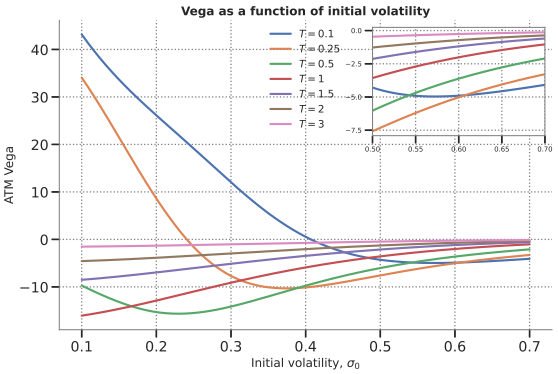

(d) Vega of double barrier option

Figure 9. This figure displays at-the-money deltas (panels (a,b)) and vegas (panels (c,d)) of the single barrier option price with $H = 80$ (panels (a,c)) and the double barrier option price with $H_1 = 70 < H_2 = 130$ (panels (b,d)) both as functions of σ_0 for different maturities T. The inner window magnifies the effects over a selected range. The dynamics of X are given by the Heston model. The parameters are $r = 0.05$, $\delta = 0.02$, $\kappa = 2$, $\theta = 0.09$, $\eta = 0.4$, $\rho = 0$, $X_0 = 100$, $K = 100$.

7. Conclusions

In this paper we developed a new approach to compute the prices and deltas of double barrier knock-out options written on assets with stochastic (diffusion) volatility. A characterization of the option price involving an early knock-out discount was derived based on the local time-space formula of Peskir. This characterization led to a system of coupled Volterra integral equations of the first kind for the deltas of the option at the upper and lower barriers. An algorithm for computation, based on quasi-Monte Carlo simulation and a Brownian bridge construction, was then proposed and shown to converge numerically to the true value of the claim when the underlying price follows a geometric Brownian motion. A numerical study illustrated properties of knock-out call option prices in the Heston volatility model with respect to the coefficients of the volatility process.

We found that double barrier option prices and deltas behave fundamentally differently from single barrier option prices and deltas. One of the most significant results is that the double barrier option delta

at the lower barrier displays a non-monotonic behavior over time, increasing at sufficiently long times-to-maturity, then decreasing as the maturity date approaches. In comparison the single barrier option delta at the barrier falls over time before vanishing. These patterns apply when volatility is constant, as in the Black-Scholes-Merton model. While the general patterns are similar under the MRSRV model, there are also stochastic variations associated with volatility innovations. In our numerical experiments, these fluctuations have a limited impact on the deltas of long-dated ATM double barrier contracts, but the impact can become substantial at shorter maturities. As documented, the responses of single and double barrier option prices to changes in the coefficients of the volatility process are also significantly different and they typically depend on time-to-maturity in the case of double barrier options. Taken together, these results underline the fact that intuitions based on the behavior of single barrier option prices and deltas cannot be extrapolated to double barrier contracts. Effective risk management of barrier options therefore requires specialized knowledge of the contract concerned and tailoring to the prevailing environment.

The methods developed in the paper are of interest to buyers and sellers of single and double barrier knock-out options. The numerical results shed light on the intrinsic properties of deltas and prices in markets with stochastic volatility, enhancing our knowledge of these financial instruments. The valuation formulas derived can be used to design effective investment and risk management strategies tailored to the relevant contract and market environment.

Author contributions

Jerome Detemple : Methodology, Conceptualization, Writing; Yerkin Kitapbayev: Methodology, Conceptualization, Writing; Danila Shabalin: Methodology, Conceptualization, Writing, Software, Visualization. All authors have read and approved the final version of the manuscript for publication.

Use of Generative-AI tools declaration

The authors declare they have not used Artificial Intelligence (AI) tools in the creation of this article.

Acknowledgments

Y. Kitapbayev is supported by the Khalifa University of Science and Technology under grant number FSU-2023- 013. We thank Alex Lipton and Goran Peskir for helpful discussions.

Conflict of interest

All authors declare no conflicts of interest in this paper.

References

1. G. Agazzotti, J. P. Aguilar, C. Aglieri Rinella, J. L. Kirkby, Calibration and option pricing with stochastic volatility and double exponential jumps, *J. Comput. Appl. Math.*, **465** (2025), 116563. https://doi.org/10.1016/j.cam.2025.116563

2. K. E. Atkinson, An existence theorem for Abel integral equations, *SIAM J. Math. Anal.*, **5** (1974), 729–736. https://doi.org/10.1137/0505071

3. D. S. Bates, Jumps and stochastic volatility: Exchange rate processes implicit in deutsche mark options, *Rev. Financ. Stud.*, **9** (1996), 69–107. https://doi.org/10.1093/rfs/9.1.69

4. M. Boyarchenko, S. Levendorski, Valuation of continuously monitored double barrier options and related securities, *Math. Financ.*, **22** (2012), 419–444. http://doi.org/10.1111/j.1467-9965.2010.00469.x

5. H. Brunner, *Collocation methods for Volterra integral and related functional equations*, Cambridge: Cambridge University Press, 2004. https://doi.org/10.1017/CBO9780511543234

6. R. E. Caflisch, B. Moskowitz, Modified Monte Carlo methods using quasi-random sequences, In: *Monte Carlo and Quasi-Monte Carlo Methods in Scientific Computing. Lecture Notes in Statistics, Springer, New York*, 1995. https://doi.org/10.1007/978-1-4612-2552-2_1

7. P. Carr, A. Itkin, Semi-closed form solutions for barrier and American options written on a time-dependent Ornstein-Uhlenbeck process, *J. Deriv.,* **29** (2021), 9–26. https://doi.org/10.3905/jod.2021.1.133

8. P. Carr, A. Itkin, D. Muravey, Semi-closed form prices of barrier options in the time-dependent CEV and CIR models, *J. Deriv.*, **28** (2020), 26–50. https://doi.org/10.3905/jod.2020.1.113

9. P. Carr, A. Itkin, D. Muravey, Semi-analytical pricing of barrier options in the time-dependent Heston model, *J. Deriv.*, **30** (2022), 141–171. https://doi.org/10.3905/jod.2022.30.2.141

10. H. Chi, P. Beerli, D. W. Evans, M. Mascagni, On the scrambled Sobol sequence, In: *International Conference on Computational Science, Berlin: Springer*, 2005, 775–782. https://doi.org/10.1007/11428862_105

11. C. Chiarella, B. Kang, G. H. Meyer, The evaluation of barrier option prices under stochastic volatility, *Comput. Math. Appl.*, **64** (2012). 2034–2048. https://doi.org/10.1016/j.camwa.2012.03.103

12. J. Detemple, Y. Kitapbayev, The valuation of corporate securities with finite maturity debt, *IMA J. Manag. Math.*, in press, 2025. https://doi.org/10.1093/imaman/dpaf028

13. H. Funahashi, T. Higuchi, An analytical approximation for single barrier options under stochastic volatility models, *Ann. Oper. Res.*, **266** (2018), 129–157. http://doi.org/10.1007/s10479-017-2559-3

14. H. Geman, M. Yor, Pricing and hedging double-barrier options: A probabilistic approach, *Math. Financ.*, **6** (1996), 365–378. https://doi.org/10.1111/j.1467-9965.1996.tb00122.x

15. C. Guardasoni, S. Sanfelici, Fast numerical pricing of barrier options under stochastic volatility and jumps, *SIAM J. Appl. Math.*, **76** (2016), 27–57. https://doi.org/10.1137/15100504X

16. C. Guardasoni, M. R. Rodrigo, S. Sanfelici, A Mellin transform approach to barrier option pricing, *IMA J. Manag. Math.*, **31** (2020), 49–67. https://doi.org/10.1093/imaman/dpy016

17. T. Guillaume, Analytical valuation of a general form of barrier option with stochastic interest rate and jumps, *Rev. Deriv. Res.*, **28** (2025), 8. https://doi.org/10.1007/s11147-025-09215-6

18. M. Ha, D. Kim, J. H. Yoon, Pricing of timer volatility-barrier options under Heston's stochastic volatility model, *J. Comput. Appl. Math.*, **457** (2025), 116310. https://doi.org/10.1016/j.cam.2024.116310

19. S. L. Heston, A closed-form solution for options with stochastic volatility with applications to bond and currency options, *Rev. Financ. Stud.*, **6** (1993), 327–343. https://doi.org/10.1093/rfs/6.2.327

20. J. Hull, A. White, The pricing of options on assets with stochastic volatilities, *J. Financ.*, **42** (1987), 281–300. https://doi.org/10.1111/j.1540-6261.1987.tb02568.x

21. A. Itkin, D. Muravey, Semi-closed form prices of barrier options in the Hull-White model, preprint paper, 2004. https://doi.org/10.48550/arXiv.2004.09591

22. A. Itkin, D. Muravey, Semi-analytic pricing of double barrier options with time-dependent barriers and rebates at hit, *Front. Math. Financ.*, **1** (2022), 53–79. https://doi.org/10.3934/fmf.2021002

23. J. Jeon, J. H. Yoon, C. R. Park, An analytic expansion method for the valuation of double-barrier options under a stochastic volatility model, *J. Math. Anal. Appl.*, **449** (2017), 207–227. https://doi.org/10.1016/j.jmaa.2016.11.061

24. D. Kim, J. H. Yoon, C. R. Park, Pricing external barrier options under a stochastic volatility model, *J. Comput. Appl. Math.*, **394** (2021), 113555. https://doi.org/10.1016/j.cam.2021.113555

25. J. L. Kirkby, C. A. Rinella, J. P. Aguilar, N. Rupprecht, Return to the barrier: Option pricing and calibration in foreign exchange markets, *J. Risk*, **27** (2025), 1–32. http://doi.org/10.21314/JOR.2025.005

26. A. Kufner, B. Opic, How to define reasonably weighted Sobolev spaces, *Comment. Math. Univ. Carolin.*, **25** (1984), 537–554.

27. N. Kunimoto, M. Ikeda, Pricing options with curved boundaries, *Math. Financ.*, **2** (1992), 275–298. http://doi.org/10.1111/j.1467-9965.1992.tb00033.x

28. M. K. Lee, J. H. Kim, Pricing vanilla, barrier, and lookback options under two-scale stochastic volatility driven by two approximate fractional Brownian motions, *AIMS Math.*, **9** (2024), 25545–25576. http://doi.org/10.3934/math.20241248

29. P. Linz, *Analytical and numerical methods for Volterra equations*, Philadelphia: SIAM, 1985. http://doi.org/10.1137/1.9781611970852

30. A. Lipton, *Mathematical methods for foreign exchange: A financial engineer's approach*, Singapore: World Scientific, 2001. http://doi.org/10.1142/4694

31. A. Lipton, A. Sepp, Toward an efficient hybrid method for pricing barrier options on assets with stochastic volatility, *Wilmott*, **121** (2022), 74–88. http://doi.org/10.54946/wilm.11053

32. C. F. Lo, C. H. Hui, Valuing double-barrier options with time-dependent parameters by Fourier series expansion, *IAENG Int. J. Appl. Math.*, **36** (2007), 1–5.

33. G. Loeper, O. Pironneau, A mixed PDE/Monte-Carlo method for stochastic volatility models, *CR Acad. Sci. I-Math.*, **347** (2009), 559–563. http://doi.org/10.1016/j.crma.2009.02.021

34. R. C. Merton, Theory of rational option pricing, *Bell J. Econ.*, **4** (1973), 141–183. https://doi.org/10.2307/3003143

35. A. Mijatović, Local time and the pricing of time-dependent barrier options, *Financ. Stoch.*, **14** (2010), 13–48. https://doi.org/10.1007/s00780-008-0077-5

36. A. Mijatović, M. Pistorius, Continuously monitored barrier options under Markov processes, *Math. Financ.*, **23** (2013), 1–38. https://doi.org/10.1111/j.1467-9965.2011.00486.x

37. A. Pelsser, Pricing double barrier options using Laplace transforms, *Financ. Stoch.*, **4** (2000), 95–104. https://doi.org/10.1007/s007800050005

38. G. Peskir, A change-of-variable formula with local time on curves, *J. Theor. Probab.*, **18** (2005), 499–535. https://doi.org/10.1007/s10959-005-3517-6

39. G. Peskir, On the American option problem, *Math. Financ.*, **15** (2005), 169–181. https://doi.org/10.1111/j.0960-1627.2005.00214.x

40. G. Peskir, A. Shiryaev, Optimal stopping and free-boundary problems, In: *Lectures in Mathematics, ETH Zürich, Birkhäuser Basel*, 2006. https://doi.org/10.1007/978-3-7643-7390-0

41. QuantLib: a free/open-source library for quantitative finance, Version v1.39, 2025. https://doi.org/10.5281/zenodo.1440997

42. S. Shahmorad, M. Mostafazadeh, Existence, uniqueness and regularity of the solution for a system of weakly singular Volterra integral equations of the first kind, *J. Integral Equ. Appl.*, **35** (2023), 105–117. https://doi.org/10.1216/jie.2023.35.105

43. R. Weiss, Product integration for the generalized Abel equation, *Math. Comp.*, **26** (1972), 177–190. https://doi.org/10.1090/s0025-5718-1972-0299001-7

44. G. A. Willard, Calculating prices and sensitivities for path-independent derivatives securities in multifactor models, *J. Deriv.*, **5** (1997), 45–61. https://doi.org/10.3905/jod.1997.407982

45. U. Wystup, *FX options and structured products*, Hoboken: John Wiley & Sons, 2006. https://doi.org/10.1002/9781118673355

46. S. Zhang, J. Zhao, Efficient simulation for pricing barrier options with two-factor stochastic volatility and stochastic interest rate, *Math. Probl. Eng.*, (2017), 3912036. https://doi.org/10.1155/2017/3912036

47. Y. X. Zhao, J. Y. Bao, Barrier option pricing in regime switching models with rebates, *Acta Math. Appl. Sin., Engl.*, **40** (2024), 849–861. https://doi.org/10.1007/s10255-024-1053-3

Appendix

A. Proofs of Theorems 2.1 and 2.2.

Since the down-and-out option price function $V \in C^{1,2}$ on $[0,T)\times(H,\infty)$ and $V(t,x)=0$ for $x \le H$, we can apply Peskir's local time-space formula (see [38, 40]) to $e^{-r(T-t)}V(T,X_T)$ in order to obtain

$$\begin{aligned} e^{-r(T-t)}V(T,X_T) =& V(t,x) + \int_t^T e^{-r(u-t)}(V_t + \mathbb{L}V - rV)(u,X_u)du \\ &+ M_T + \frac{1}{2}\int_t^T e^{-r(u-t)}V_x(u,H+)d\ell_u^H(X) \end{aligned} \tag{A.1}$$

where M is a zero-mean martingale and $\ell^H(X)$ is the local time of X at H:

$$\ell_s^H(X) := Q - \lim_{\varepsilon \downarrow 0} \frac{1}{2\varepsilon} \int_0^s I(H-\varepsilon < X_u < H+\varepsilon) d\langle X \rangle_u . \tag{A.2}$$

Now by taking the expected value on both sides, using PDE (2.6), the optional sampling theorem, the terminal condition for V, the boundary condition at H, and inserting $x = H+$, we obtain

$$\mathbb{E}_{t,H}[e^{-r(T-t)}(X_T - K)^+] = \frac{1}{2} \int_t^T e^{-r(u-t)} V_x(u, H+) \mathbb{E}_{t,H}[d\ell_u^H(X)]$$

for $t \in [0, T]$ or

$$V_e(t, H) = \frac{1}{2} \int_t^T e^{-r(u-t)} \varphi\left(d^-(H, H, u-t)\right) \frac{\sigma H}{\sqrt{u-t}} V_x(u, H+) du$$

where φ is the standard normal pdf and the function d^- was given in (2.11). For an Itô process, the expected increment of the local time at H equals one half of the local variance at H times the transition density at H; the kernel already reflects this proportionality. This gives us a linear Volterra equation of the first kind for $V_x(t, H+)$. Once we recover $V_x(t, H+)$, we can compute the barrier option premium as

$$V(t, x) = \mathbb{E}_{t,x}[e^{-r(T-t)}(X_T - K)^+] - \frac{1}{2} \int_t^T e^{-r(u-t)} V_x(u, H+) K(t, x; u) du \tag{A.3}$$

where $K(t, x; u) = \varphi\left(d^-(x, H, u-t)\right) \frac{\sigma H}{\sqrt{u-t}}$.

B. Proofs of Theorems 5.1 and 5.2.

As for Theorems 2.1 and 2.2, we employ the local time-space formula of [38] for $e^{-\int_t^T r(s)ds} V(T, X_T)$:

$$\begin{aligned} e^{-\int_t^T r(s)ds} V(T, X_T) =& V(t, x) + \int_t^T e^{-\int_t^u r(s)ds} (V_t + \mathbb{L}V - rV)(u, X_u) du \\ &+ M_T + \frac{1}{2} \int_t^T e^{-\int_t^u r(s)ds} V_x(u, H_1+) d\ell_u^{H_1}(X) \\ &- \frac{1}{2} \int_t^T e^{-\int_t^u r(s)ds} V_x(u, H_2-) d\ell_u^{H_2}(X) \end{aligned} \tag{B.1}$$

where M is the zero-mean martingale and $\ell^{H_i}(X)$ is the local time of X at H_i, $i = 1, 2$. Now we take the expected value on both sides, and use Eq (5.3), the optional sampling theorem, the terminal condition for V, and the definition (5.8) of the auxiliary contract value V_0, and obtain the double barrier option price as

$$\begin{aligned} V(t, x) =& V_0(t, x) - \frac{1}{2} \int_t^T e^{-\int_t^u r(s)ds} V_x(u, H_1+) \mathbb{E}_{t,x}[d\ell_u^{H_1}(X)] \\ &+ \frac{1}{2} \int_t^T e^{-\int_t^u r(s)ds} V_x(u, H_2-) \mathbb{E}_{t,x}[d\ell_u^{H_2}(X)] \end{aligned} \tag{B.2}$$

$$= V_0(t,x) - \frac{1}{2}\int_t^T e^{-\int_t^u r(s)ds} V_x(u,H_1+)\varphi\left(d^-(x,H_1,t,u)\right)\frac{\sigma^2(u)H_1}{\sqrt{\int_t^u \sigma^2(s)ds}}du$$
$$+ \frac{1}{2}\int_t^T e^{-\int_t^u r(s)ds} V_x(u,H_2-)\varphi\left(d^-(x,H_2,t,u)\right)\frac{\sigma^2(u)H_2}{\sqrt{\int_t^u \sigma^2(s)ds}}du.$$

Next we insert $x = H_1+$ and $x = H_2-$, respectively, on both sides of (B.2). This will give us the system of coupled linear Volterra equations of the first kind (5.9) and (5.10) for $f_1(t) = V_x(t,H_1+)$ and $f_2(t) = V_x(t,H_2-)$, $t \in [0,T)$.

AIMS Press